

The electronic structure change with Gd doping of Hf O 2 on silicon

Ya. B. Losovyj, Ihor Ketsman, A. Sokolov, K. D. Belashchenko, P. A. Dowben, Jinke Tang, and Zhenjun Wang

Citation: [Applied Physics Letters](#) **91**, 132908 (2007); doi: 10.1063/1.2787967

View online: <http://dx.doi.org/10.1063/1.2787967>

View Table of Contents: <http://scitation.aip.org/content/aip/journal/apl/91/13?ver=pdfcov>

Published by the [AIP Publishing](#)

Articles you may be interested in

[Formation of the dopant-oxygen vacancy complexes and its influence on the photoluminescence emissions in Gd-doped HfO₂](#)

J. Appl. Phys. **116**, 123505 (2014); 10.1063/1.4896371

[First-principles study of the structural, electronic, and optical properties of Y-doped SrSi₂](#)

J. Appl. Phys. **113**, 043515 (2013); 10.1063/1.4788715

[Band structure and electrical properties of Gd-doped HfO₂ high k gate dielectric](#)

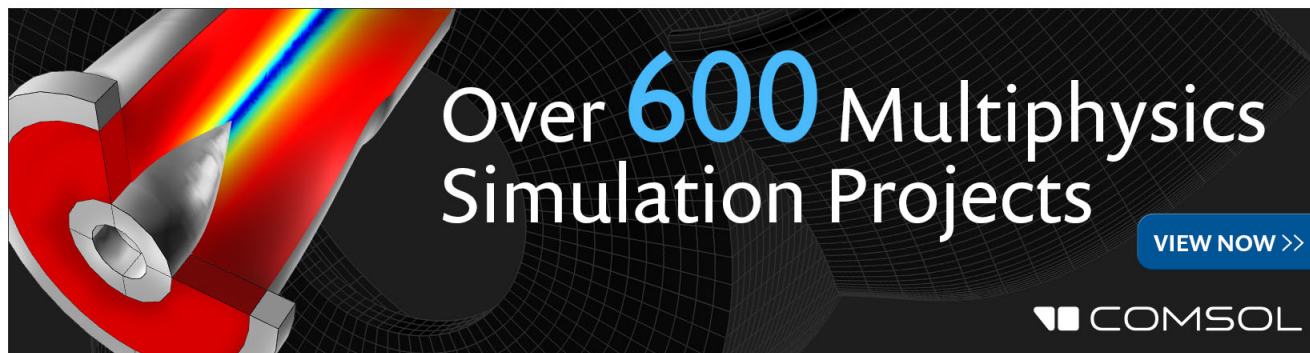
Appl. Phys. Lett. **97**, 012901 (2010); 10.1063/1.3460277

[Band structures, magnetic properties, and enhanced magnetoresistance in the high pressure phase of Gd and Y doped two-dimensional perovskite Sr₂CoO₄ compounds](#)

Appl. Phys. Lett. **91**, 062501 (2007); 10.1063/1.2759273

[Nitrogen doping and thermal stability in Hf Si O x N y studied by photoemission and x-ray absorption spectroscopy](#)

Appl. Phys. Lett. **87**, 182908 (2005); 10.1063/1.2126112

The advertisement features a 3D cutaway of a mechanical part with a rainbow-colored stress or temperature distribution. The text 'Over 600 Multiphysics Simulation Projects' is prominently displayed in white and blue. A blue button with white text says 'VIEW NOW >>'. The COMSOL logo is in the bottom right corner.

Over **600** Multiphysics
Simulation Projects

[VIEW NOW >>](#)

COMSOL

The electronic structure change with Gd doping of HfO₂ on silicon

Ya. B. Losovyj

Center for Advanced Microstructures and Devices, Louisiana State University, 6980 Jefferson Highway, Baton Rouge, Louisiana 70806, USA

Ihor Ketsman, A. Sokolov, K. D. Belashchenko, and P. A. Dowben^{a)}

Department of Physics and Astronomy, University of Nebraska-Lincoln, P.O. Box 880111, Lincoln, Nebraska 68588-0111, USA

Jinke Tang and Zhenjun Wang

Department of Physics and Astronomy, University of Wyoming, Laramie, Wyoming 82071, USA

(Received 16 July 2007; accepted 31 August 2007; published online 26 September 2007)

Gd-doped HfO₂ films deposited on silicon substrates undergo a crystallographic change from monoclinic to fluorite (cubic) phase with increasing Gd concentrations. The crystallographic phase change is accompanied by a small increase in the valence bandwidth and in the apparent band offset in the surface region. Electrical measurements show pronounced rectification properties for lightly doped Gd:HfO₂ films on *p*-Si and for heavily-doped Gd:HfO₂ films on *n*-Si, suggesting a crossover from *n*-type to *p*-type behavior with increasing doping level. © 2007 American Institute of Physics. [DOI: 10.1063/1.2787967]

While HfO₂ has attracted considerable attention as a high- κ dielectric oxide,^{1,4} the cubic phase of yttrium doped HfO₂ appears to have improved dielectric properties.⁵ It has been demonstrated that Y₂O₃ doping stabilizes HfO₂ in the cubic phase.^{5–8} Doping of HfO₂ by Er,^{7–9} Gd,^{8,10,11} and many other rare earth elements⁸ also induces a monoclinic to cubic phase transition. The gadolinium doping of a number of wide band gap semiconductors^{12–14} suggested that Gd doping of HfO₂ may lead to a dilute magnetic semiconductor.^{15,16} Moreover, semiconducting Gd-doped HfO₂ may provide a promising new class of materials for neutron detection technologies.¹⁷

At 3% Gd substitution for Hf in HfO₂, Gd contributes to the density of states at 9.5–10.5 eV binding energy, as demonstrated by resonant photoemission.^{17,18} The lattice remains in the monoclinic phase,^{16,17} which is strained by about 3%.¹⁷ Here, we show that further doping leads to a structural phase change with subtle changes in the electronic structure.

The Gd-doped HfO₂ films were deposited on both *p*-type and *n*-type single crystal Si(100) substrates using pulsed laser deposition at a growth rate of about 0.15 Å/s. The Gd-HfO₂ target was prepared by standard ceramic techniques using HfO₂ and Gd₂O₃ powders, as described elsewhere.^{16,17} The films were deposited at a substrate temperature of 500 °C. The deposition was carried out in a mixture of H₂ and Ar (8% H₂) to introduce oxygen vacancies, and the vacuum was maintained at 10^{–5} Torr during the deposition. The doping level was determined from the target composition and confirmed by companion near edge x-ray absorption spectroscopy (NEXAFS) and by x-ray emission spectroscopy on separate similarly prepared samples. (Throughout, *x*% Gd means the nominal composition Hf_{1–*x*}Gd_{*x*}O_{2–0.5*x*}.) The NEXAFS and EXAFS data indicate that the Gd atoms occupy the Hf sites in the Gd-doped HfO₂ films.

X-ray diffraction (XRD) patterns show that the resulting HfO₂ films with 3% Gd, which are approximately 250 nm

thick, are in the single monoclinic phase with strong texture growth and about 3% strain compared to the undoped HfO₂ (Fig. 1), consistent with prior results.¹⁷ With increased doping levels, a new phase is evident, as seen from the x-ray diffraction patterns in Fig. 1. For 10% Gd doping levels, this new phase retains a minority monoclinic phase component, but for 15% Gd doping, the films are free of the monoclinic phase, i.e. stable. This new phase, apparent with the more highly Gd-doped HfO₂ films, is consistent with the fcc fluorite phase in XRD, as is expected.^{8–10} The presence of a small amount of the Gd₂Hf₂O₇ pyrochlore phase cannot, *a priori*, be excluded, because it differs from fluorite only in the presence of ordering within the cation sublattice.^{8,11}

To determine the placement of the Fermi level, temperature-dependent angle-resolved photoemission experiments were performed using the 3 m toroidal grating monochromator beam line in an UHV chamber previously described.^{18,19} The Fermi level (E_F) was established from a

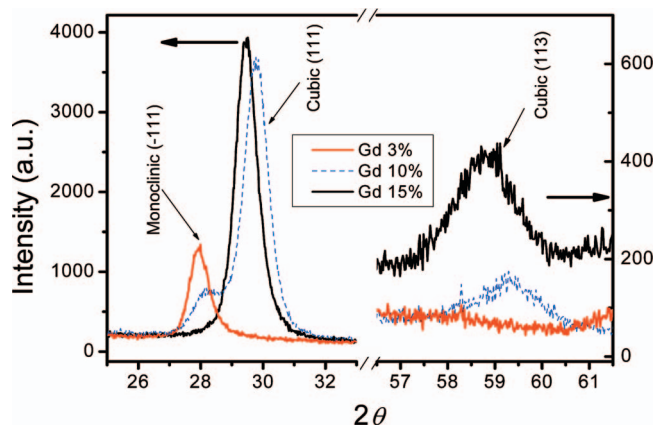


FIG. 1. (Color) Part of the XRD pattern for 3%, 10%, and 15% Gd doped HfO₂. The 3% Gd doped films are consistent with that of the HfO₂ in a simple monoclinic structure. The 10% doped samples are mixed monoclinic and majority cubic phases, as indicated, while 15% Gd-doped samples are in a fluorite phase. In the fluorite fcc phase, the lattice constant increases with increased Gd doping.

^{a)}Electronic mail: pdowben@unl.edu

gold film in electrical contact with the sample, and a very careful effort was undertaken to eliminate and exclude charging effects from the photoemission measurements of Gd-doped HfO_2 films. Photoemission was undertaken over a range of temperatures 100–700 K, but the data presented here were taken at 320 °C, where surface charging was found to be negligible. This is well below the temperature dependent structural phase transition 700 °C.

From Fig. 2, it is clear that the valence band edge is placed well away from the Fermi level for both Gd-doped and undoped HfO_2 films. The Hf 4*f* binding energies of 18–21 eV are substantially larger than those reported by Renault *et al.*,²⁰ Hf 4*f* binding energies and valence band edge are similar⁶ or slightly larger than those reported elsewhere.^{21–23} As seen in Fig. 2, the Hf 4*f* binding energies increase when Gd doping is increased from 3% to 10%.

The increase with Gd doping in the intensity of the photoemission features in the oxygen 2*p* region of the valence band, at 5–10 eV binding energy, relative to the Hf 4*f* features at 18–21 eV binding energies, suggests that Gd 4*f* states contribute to the shoulder on the broad photoemission peak at the binding energy of 9–10 eV. This contribution was confirmed by resonant photoemission studies of lightly doped Gd: HfO_2 films,^{17,18} which showed that the photoelectron intensity from this shoulder is strongly enhanced at about 148 eV photon energy.^{17,18} As seen in the upper inset of Fig. 2, theoretical calculations (see below) suggest that the phase transition from monoclinic to fluorite phase is also accompanied by a transfer of the oxygen spectral weight toward this shoulder, which makes it difficult to assign these intensity changes precisely.

With Gd doping, there is also an increase in the small density of states between 4 eV binding energy and the Fermi level, as seen in the lower inset of Fig. 2. In this region, the density of states suggested by photoemission decreases with increasing yttrium doping levels,⁶ but is seen here to increase with Gd doping. Indeed, the increase in binding energy of all the major photoemission features seen with Gd doping is not observed for $(\text{HfO}_2)_{1-x}(\text{Y}_2\text{O}_3)_x$ samples.⁶ The possibility of surface defects or surface states pinning the Fermi level differently for the two different dopants (Y and Gd) cannot be excluded and may in fact be likely. Yttrium segregates away from the surface of zirconia,²⁴ and may behave similarly with HfO_2 , while gadolinium, because of its larger size, should segregate toward the surface; although for the samples studied here, significant gadolinium surface segregation was not observed. Thus, even with nominally similar surface terminations,²⁵ the surface Fermi level pinning may be very different for the two dopants.

The assignment of the photoemission features was verified by first-principles electronic structure calculations using the full-potential linear augmented plane-wave method in the local density approximation. Excitations involving the 4*f* shell of Gd or Hf were treated using the core-hole method, as described previously.¹⁷ As reported previously,¹⁷ the calculated Gd photoemission binding energy in the fluorite phase is 5.5 eV below the valence band maximum. Placing the valence band maximum at about 4 eV below the Fermi level, this results in a 9.5 eV binding energy for the Gd 4*f* states with respect to the Fermi level, in agreement with resonant photoemission data.^{17,18} To place this in context, the Gd 4*f* binding energies for the gadolinium oxide are from 8.5 to 11 eV binding energies with respect to the Fermi

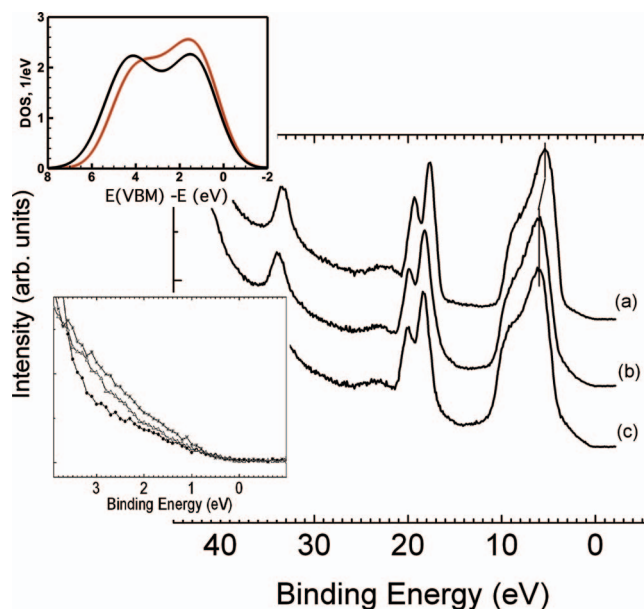


FIG. 2. (Color) Different band intensities for (a) pristine: 0%, (b) 3%, and (c) 15% Gd-doped films of HfO_2 . The photon energy is 70 eV and the light incidence angle is 45°. The increasing contributions to the density of states near to the Fermi level are illustrated in the inset for 0% (black dots), 3% (open triangles), and 15% (stars) Gd doping levels in the inset at the bottom left, while the calculated density of states for the fluorite (black) and the monoclinic (red) phases of pure HfO_2 , in the region of the valence band maximum (the O 2*p* bands) are shown in the upper left inset.

level, with smaller binding energies with respect to the valence band maximum than observed here.²⁶

Similarity of the photoemission intensities (Fig. 2) for monoclinic and fluorite phases of HfO_2 reflects the similarity of the electronic structure. In particular, the upper inset in Fig. 2 shows the calculated valence band density of states (DOS) convoluted with a Gaussian of 0.8 eV width for the two phases of pure HfO_2 . Although the bandwidth is almost 1 eV larger for the fluorite phase (6.5 eV compared to 5.6 eV in the monoclinic phase), the DOS at the band bottom is small. Therefore, if the finite linewidth is taken into account, the apparent bandwidth increases by less than 0.5 eV. This generally agrees with the observed photoemission valence bandwidths, if the peak is resolved into a sum of Gd 4*f* peak and pure oxygen *p* band, and the tailing density of states toward the Fermi level is neglected, as seems to often be the practice.⁶

Further, we calculated the Hf 4*f* excitation energies using the core-hole method for both the fluorite and the monoclinic phases. In both cases, we used a unit cell with four Hf and eight O atoms and changed the 4*f* occupation from 14 to 13 on one of the Hf atoms (the excited core is spin polarized and the calculations are done including the valence band spin polarization self-consistently). The core is treated fully relativistically, and the hole is placed on the 4*f*_{7/2} level which has lower binding energy within the 4*f* doublet. The excited electron fills a donor level which lies at about 0.6 eV below the conduction band minimum (the level is broadened due to the finite size of the supercell). Estimating the distance from this level to the valence band maximum and subtracting it from the energy difference between the photoexcited 4*f*¹³ and the ground 4*f*¹⁴ states, we find the Hf 4*f*_{7/2} photoexcitation energy of 14.4 eV for the fluorite phase and 14.1 eV for the monoclinic phase. The 0.3 eV difference lies within the

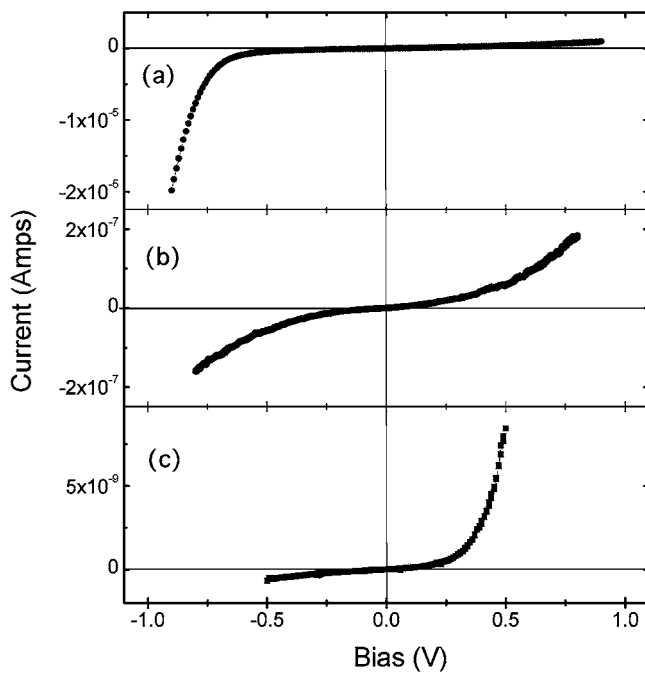


FIG. 3. Heterojunction diodes constructed Gd-doped HfO_2 on silicon. With oxygen vacancies, the 3% Gd-doped HfO_2 is over compensated and forms a rectifying diode on p -type silicon (a). The 10% Gd-doped HfO_2 is not overcompensated by oxygen vacancies and does not form a rectifying diode on p -type silicon (b) but does do so on n -type silicon (c).

error associated with the finite supercell size. According to these results, the $4f$ photoemission peak should not shift appreciably relative to the valence band maximum at the transition from monoclinic to fluorite phase. We also found that the position of the Hf $4f$ photoemission peak relative to the valence band maximum is insensitive to the presence of uncompensated Gd (this was done using the same supercell with 25% Gd substitution; the excited electron then fills the valence band). All these results are consistent with Fig. 2.

p - n heterojunction diodes can be formed with strongly textured monoclinic and fluorite Gd-doped HfO_2 on Si(100). We fabricated several diodes to illustrate that the overcompensation of the expected Gd acceptor states, by oxygen vacancies, as is seen with smaller (3 at. %) Gd doping levels is not sustained at the higher Gd doping levels. An n -type band offset of the lightly Gd-doped HfO_2 relative to p -type silicon is indicated by the excellent diode rectification seen for a heterojunction of 3% Gd-doped HfO_2 and p -type silicon, as shown in Fig. 3. For the 10% Gd: HfO_2/p -Si heterojunction, no rectification or diodelike characteristics are seen, but for the 10% Gd-doped HfO_2 to n -type silicon heterojunction, we do observe rectification or diodelike characteristics, shown in Fig. 3. While these data do not conclusively show the dominant carrier, they suggest that oxygen vacancies can overcompensate the Gd acceptor states without completely destroying the semiconductor properties for 3% Gd doping levels but not for 10% Gd doping levels or higher.

The authors acknowledge insightful discussions with Alex Igantov, Andre Petukhov, and J. Brand. This work was supported by the Office of Naval Research (Grant No. N00014-06-1-0616), the Defense Threat Reduction Agency (Grant No. HDTRA1-07-1-0008), and the Nebraska Research Initiative.

- ¹M. McCoy, Chem. Eng. News **83**, 26 (2005).
- ²B. H. Lee, L. Kang, W.-J. Qi, R. Nieh, K. Onishi, and J. C. Lee, Tech. Dig. - Int. Electron Devices Meet. **1999**, 133 (1999).
- ³M. Gutowski, J. E. Jaffe, C.-L. Liu, M. Stoker, R. I. Hegde, R. S. Raj, and P. J. Tobin, Appl. Phys. Lett. **80**, 1897 (2002).
- ⁴K. P. Bastos, J. Morais, L. Miotti, R. P. Pezzi, G. V. Soares, I. J. R. Baumvol, R. I. Hegde, H. H. Tseng, and P. J. Tobin, Appl. Phys. Lett. **81**, 1669 (2002).
- ⁵Z. K. Yang, W. C. Lee, Y. J. Lee, P. Chang, M. L. Huang, M. Hong, C. H. Hsu, and J. Kwo, Appl. Phys. Lett. **90**, 152908 (2007).
- ⁶M. Komatsu, R. Yasuhara, H. Takahashi, S. Toyoda, H. Kumigashira, M. Oshima, D. Kukuruznyak, and T. Chikyow, Appl. Phys. Lett. **89**, 172107 (2006).
- ⁷J. Wang, H. P. Li, and R. Stevens, J. Mater. Sci. **27**, 5397 (1992).
- ⁸V. V. Kharton, A. A. Yaremchenko, E. N. Naumovich, and F. M. B. Marques, J. Solid State Electrochem. **4**, 243 (2000).
- ⁹P. Duran, C. Pasual, J. P. Coutures, and S. R. Skaggs, J. Am. Ceram. Soc. **66**, 101 (1983).
- ¹⁰S. L. Dole, O. Hunter, Jr., and F. W. Calderwood, J. Am. Ceram. Soc. **63**, 136 (1980).
- ¹¹S. V. Ushakov, A. Navrotsky, and K. B. Helean, J. Am. Ceram. Soc. **90**, 1171 (2007).
- ¹²S. Dhar, O. Brandt, M. Ramsteiner, V. F. Sapega, and K. H. Ploog, Phys. Rev. Lett. **94**, 037205 (2005).
- ¹³S. Dhar, T. Kammermeier, A. Ney, L. Pérez, K. H. Ploog, A. Melnikov, and A. D. Wieck, Appl. Phys. Lett. **89**, 062503 (2006).
- ¹⁴K. Potzger, S.-Q. Zhou, F. Eichhorn, M. Helm, W. Skorupa, A. Mücklich, J. Fassbender, T. Herrmannsdorfer, and A. Bianchi, J. Appl. Phys. **99**, 063906 (2006).
- ¹⁵M. Venkatesan, C. B. Fitzgerald, and J. D. M. Coey, Nature (London) **430**, 630 (2004).
- ¹⁶W. Wang, Y. Hong, M. Yu, B. Rout, G. A. Glass, and J. Tang, J. Appl. Phys. **99**, 08M117 (2006).
- ¹⁷I. Ketsman, Ya. B. Losovyj, A. Sokolov, J. Tang, Z. Wang, K. D. Belashchenko, and P. A. Dowben, Appl. Phys. A: Mater. Sci. Process. **89**, 489 (2007).
- ¹⁸Ya. B. Losovyj, I. Ketsman, E. Morikawa, Z. Wang, J. Tang, and P. A. Dowben, "Optimization of the 3 m TGM beamline, at CAMD, for constant initial state spectroscopy," Nucl. Instrum. Methods Phys. Res. A (in press).
- ¹⁹P. A. Dowben, D. LaGraffe, and M. Onellion, J. Phys.: Condens. Matter **1**, 6571 (1989).
- ²⁰O. Renault, D. Samour, J.-F. Damlencourt, D. Blin, F. Martin, S. Mathon, N. T. Barrett, and P. Besson, Appl. Phys. Lett. **81**, 3627 (2002).
- ²¹S. Suzer, S. Sayan, M. M. Banaszak Holl, E. Garfunkel, Z. Hussain, and N. M. Hamdan, J. Vac. Sci. Technol. A **21**, 106 (2003).
- ²²S. Sayan, T. Emge, E. Garfunkel, X. Zhao, L. Wielunski, R. A. Bartynski, D. Vanderbilt, J. S. Suehle, S. Suzer, and M. M. Banaszak Holl, J. Appl. Phys. **96**, 7485 (2004).
- ²³S. Sayan, R. A. Bartynski, X. Zhao, E. P. Gusev, D. Vanderbilt, M. Croft, M. M. Banaszak Holl, and S. Suzer, Phys. Status Solidi B **241**, 2246 (2004).
- ²⁴A. Eichler and G. Kresse, Phys. Rev. B **69**, 045402 (2004).
- ²⁵N. V. Skorodumova, M. Baudin, and K. Hermansson, Phys. Rev. B **69**, 075401 (2004).
- ²⁶C. Schüßler-Langeheine, R. Meier, H. Ott, Z. Hu, Chandan Mazumdar, A. Yu. Grigoriev, G. Kaindl, and E. Weschke, Phys. Rev. B **60**, 3449 (1999).